Acetic Acid–Water Interaction in Solid Interfaces

ARTICLE *in* THE JOURNAL OF PHYSICAL CHEMISTRY B · JUNE 2006

Impact Factor: 3.3 · DOI: 10.1021/jp0559736 · Source: PubMed

2 AUTHORS, INCLUDING:

Stephan Bahr

SPECS Surface Nano Analysis GmbH, Berlin, …

23 PUBLICATIONS **487** CITATIONS

Acetic Acid−Water Interaction in Solid Interfaces

A. Allouche*

Physique des Interactions Ioniques et Moléculaires, Université de Provence and CNRS, Unité Mixte de Recherche N°6633, Campus de Saint Jérôme Service 242, 13397 Marseille Cedex 20, France

S. Bahr

Institut für Physik und Physikalische Technologien, Technische Universität Clausthal, D-38678 Clausthal-Zellerfeld, Germany

Received: October 19, 2005; In Final Form: January 16, 2006

The adsorption of acetic acid on a proton-ordered water ice surface is modeled using periodic plane-waves density-functional theory. The structures of acetic acid adsorbed as a monomer or oligomers, hydrated or not, are calculated through gradient optimization. The resulting quantum electronic density of states are compared to metastable impact electron spectroscopy (MIES) results and lead to selection of the most plausible structures of acetic acid on water ice. Hypotheses are formulated for the structure of the acid film growing on the ice surface including mainly cyclic dimers and hydrated forms. Adsorptions of single water molecules on acetic acid crystal surfaces are also studied after optimization of the acetic acid crystal bulk and surface structure. More comparisons with spectroscopic studies are proposed in the accompanying paper (*J. Phys. Chem. B* **2006** *110*, 8649).

I. Introduction

Ice has been the subject of a large number of contributions in the past decade because of its role in heterogeneous processes found in the interstellar medium, in planetary chemistry, and also in the atmospheric and environmental domains. As far as water ice is concerned, hydrogen bonding becomes the predominant interaction. This is specially the case when the reactive molecule's chemistry is also governed by hydrogen bonds such as carboxylic acids. Among them, acetic acid plays a special role because of its dual functional groups: hydrophilic by its carboxyl group and hydrophobic by its methyl tail. Because of this special reactivity, the physics of the interface between water (solid or liquid) and acetic acid is far from being well understood.

Acetic acid (AA) is also well known for its ability to form dimers in the gas phase,[1,2] whereas in the liquid phase or in a solution the point is not so clear.[3,4] According to Génin et al.[3] who performed an infrared and Raman spectroscopic study of aqueous solutions of acetic acid, at low concentrations the acid is largely a hydrated monomer. As acid concentration increases, the hydrated monomer is gradually replaced by a hydrated linear dimer and then by the cyclic dimer. At higher concentrations, longer oligomers coexist with cyclic dimers.

Lately, several papers have been published that were devoted to acetic acid adsorption on water ice, whether experimental[5−8] or theoretical.[9,10] Nevertheless, the adsorption mode and the relative contribution of each contributing partner are still widely being debated. The combination of infrared spectroscopy, MIES (metastable impact electron spectroscopy), UPS(HeII), and TPD (temperature-programmed spectroscopy) with quantum calculation is a powerful tool of investigation that we implemented already in the case of formic acid.[11,12] The present paper is devoted only to the quantum part of the project; for implications and comparisons with experiments readers are referred to the accompanying experiment−theory paper (Paper II[13]). However, because the MIES spectra are derived directly from the electronic density of states (DOS), a tentative comparison between quantum DOS and MIES is proposed in the present paper. But, as will be analyzed in Paper II, the FTIR analysis in the context of AA−water ice interaction is indicative only for solid AA organization. Therefore, although a large number of quantum spectra have been calculated during the present work, vibrational analysis is not evoked here.

This paper has been organized as follows: first, the adsorption of a single acetic acid on ice was considered using the solid-state DFT method taking into account the periodic boundary conditions. The adsorption of acetic acid oligomers, pure or hydrated, was studied using the same method.

Because the balance of acid−acid, acid−water, and water−water interaction at the interface has the predominant role in these processes, we have also studied the inverse adsorption, single water on acetic acid surfaces cut out of the bulk crystalline acetic acid.

II. Computational Details and Acetic Acid Structure

To represent the surface (ice or acetic acid), two general strategies are available. The molecular cluster method was implemented in our last studies; the ice surface was represented by a cluster of 6−10 hydrogen-bonded water molecules.[11] This option supports sophisticated methods and is very useful for spectroscopy applications. The downside is that the solid three-dimensional boundary conditions cannot be included and the very long computation times restrict the system to a very small number of constituents.

Another quantum method can be chosen in the domain of solid-state physics. In this case the periodic boundary conditions

* Corresponding author. E-mail: Alain.Allouche@up.univ-mrs.fr.

10.1021/jp0559736 CCC: $33.50
Published on Web 04/04/2006

are fully taken into account. The periodic three-dimensional calculations were performed within the framework of the gradient-corrected density functional theory using the PWscf computer code from the Quantum-Espresso package.[14] Exchange and correlation functionals are Perdew−Burke−Ernzerhof PBE. A plane-wave basis set was used associated to Vanderbilt ultrasoft pseudopotentials[15] and with an energy cutoff of 30 Ry (408 eV). The same method was implemented during our study on carbon monoxide adsorption on ice[16] and proved efficient even if the CO−ice interactions are very small. Of course, the plane-wave basis set does not generate any BSSE problem on the binding energy. Another advantage, useful for the comparison with MIES/UPS spectroscopy, is that the total density of states can be projected on each of the constituents, ice or acid, making the analysis much easier.

The surface of ice was represented as a two-dimensional (2D) infinite slab whose unit cell of $Pna2_1$ symmetry, containing 48 atoms, was that optimized by the Turin group.[17] This model of proton ordered ice is preferred to hexagonal ice (Ih) because the ordinary ice structure generates a dipole moment between the two slab faces, while this problem is avoided using the Turin model. The crystal cell dimensions are 7.985 × 8.935 × 20.0 Å.

The binding energy (BE) of a moiety M (AA, H_2O, ...) to the ice surface is evaluated as follows:

$$\Delta E_{BE} = E(M + H_2O) - E(M) - E(H_2O_{surface}) \qquad (1)$$

This value is also referred to in the text as "adsorption energy" or "interaction energy"; the desorption energy in this framework is simply $-\Delta E_{BE}$.

Because there is a competition between modes (pure or mixed acid−water) of adsorption, involving different numbers of molecules, a common standard must be found for quantification purposes. The cohesive energy reported is calculated as being

$$\Delta E = [\Delta E(\text{tot}) - n\Delta E(\text{AA}) - m\Delta E(H_2O)]/(n + m) \qquad (2)$$

where ΔE(tot) is the system's total energy, ΔE(AA) and $\Delta E(H_2O)$ are the gas-phase molecular energies, and n and m are the respective number of molecules making up the complex.

The AA molecule has two rotamers known as syn and anti isomers. The first one is also the most stable one by 28.9 kJ mol^{-1} and the rotational barrier between the two forms is 55.2 kJ mol^{-1} according to Gao et al.[9] Therefore, the probability of finding the anti isomer at cryogenic temperature is negligible and only the syn isomer will be considered here. It is also assumed that CH_3COOH and H_2O cannot dissociate; this is an approximation because AA can dissociate into carboxylate anion at low concentrations.[18]

Several computational studies were devoted to the acetic acid dimer structure, especially those by Adelia et al.[19] and Chocholousova et al.[2] on the C_{2h} (Figure 1) form, which is the most stable form (dimerization energy: −63.9 kJ mol^{-1}). The C_s or L"$_w$ in Génin et al.'s[3] dimer are less stable according to the references.

III. Acetic Acid Adsorption on Water Ice

A. Monomer. The structure of a single acetic acid molecule adsorbed on the water ice slab resulting from PWscf optimization is shown in Figure 2. AA is bonded to the surface through two rather equivalent hydrogen bonds (1.857 and 1.769 Å). The adsorption energy is −68.8 kJ mol^{-1}. This structure is very similar to the formic acid (FA) case described in ref 11. The B3LYP FA binding energy is not significantly different, −73.7 kJ mol^{-1}, and the H-bond lengths are very similar, 1.889 and 1.646 Å. These two calculations are of different origin, in particular FA is isolated on a cluster and AA forms a layer adsorbed on a slab, but it needs to be pointed out that because of the large cell size, the AA molecules can also be considered as isolated because the closer molecules on the surface are at 7.98 Å in the a crystallographic direction and 8.93 Å in the b direction, whereas the vacuum is large enough to ensure that the interaction in the c direction is negligible.

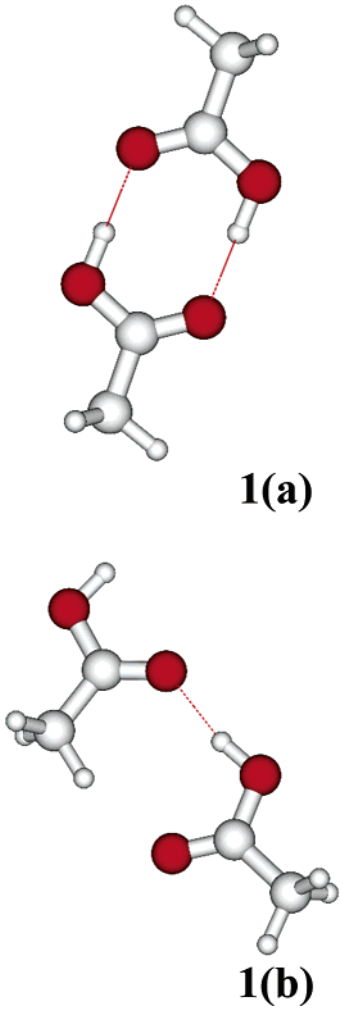

Figure 1. Syn acetic acid dimers. (a) C_{2h} dimer (b) C_s dimer.

Compoint et al.[10] have studied AA adsorption based on semiempirical potential parameters. Their results are completely consistent with ours on the monomer adsorption. They reported a double H-bond interaction (between 1.9 and 2.2 Å somewhat larger than found in our work) and an adsorption energy of −57.0 kJ mol^{-1} at 0 K.

B. Dimers and Trimers. Six structures of AA dimer adsorption were optimized without symmetry constraints (Figure 3 and Table 1). The corresponding total energies are all included in a range of 35 kJ mol^{-1}; therefore, some of these structures have a nonzero probability at sufficiently high temperatures.

In the most stable geometry ($2AA_1$), the two AA molecules are doubly bonded one to another in a slightly distorted C_{2h}-like dimer with bond lengths of 1.538 and 1.544 Å. The whole complex is bonded to the solid through two weaker H bonds of 2.074 and 2.070 Å and binding energy of −38.0 kJ mol^{-1}, this result is important for comparison with TPD.[13]

The $2AA_2$ structure is only 7.1 kJ mol^{-1} less stable (relative energies in Table 1), the two AAs are now only simply bonded

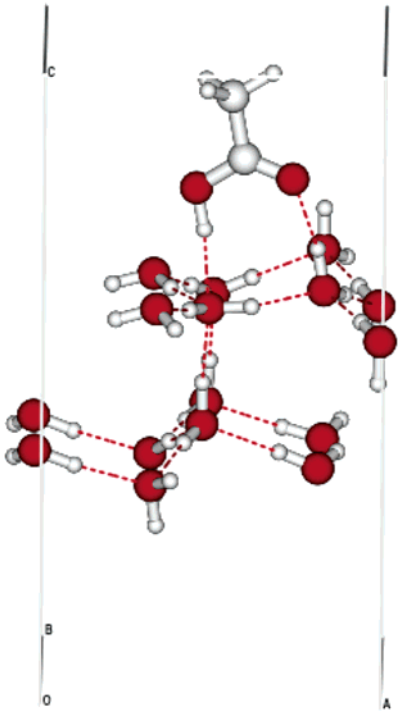

Figure 2. Acetic acid adsorption on ice using periodic PBE/PW calculation on a 16 water molecules unit cell.

(1.670 Å), and the two carboxyl groups form a dihedral angle of 65.1°. The adsystem is bonded to the surface through two H bonds of 1.927 and 1.907 Å.

$2AA_3$ is 9.5 kJ mol^{-1} higher in energy than $2AA_1$ and corresponds to two acids independently adsorbed with parallel dipole moments. $2AA_5$ (relative energy 24.4 kJ mol^{-1}) displays some similarity with the C_s dimer and Génin et al.'s L"$_w$[3] structure, it could evoke the relative orientation of two AA molecules belonging to two close catemer chains in the solid as discussed later on.

In $2AA_6$ (relative energy 34.9 kJ mol^{-1}) the two carboxyls are almost perpendicular, but the hydrogen bonds link up −C═O and H−O−C− and not the two hydroxyls like in Figure 2b of Compoint et al. optimized at the temperature of 0 K. At this point, our results are in contradiction with these authors. We claim that the most stable structure is the cyclic dimer adsorbed flat on the surface. This hypothesis is not even mentioned in their paper, but of course our open structure (which is different from theirs) is not very far in relative energy (10 kJ mol^{-1}) and must be taken into consideration. The structure most similar to theirs that we found consists of one AA completely flat on the surface and the other one almost perpendicular; it is the structure named $2AA_6$ in Figure 3, and its energy is 34.9 kJ mol^{-1} higher than $2AA_1$.

For FA,[11] our conclusions were different. The FA cyclic dimer binding energy flat on the surface was −51.2 kJ mol^{-1} (ZPE corrected) and that of the open dimer, more or less similar to $2AA_2$, −102.8 kJ mol^{-1}. We have also shown that FA coming from the gas phase could dissociate with a barrier of reaction of only 10 kJ mol^{-1} to reach the open dimer structure 23.2 kJ mol^{-1} lower in energy. Therefore, we concluded in favor of the dissociated form larger stability. It is not possible to calculate a potential energy surface using the PBE/PW tools but, even if the difference is not very important in the AA case, the most stable structure on ice corresponds to the cyclic dimer.

The most stable trimer on the ice structure ($3AA_1$ in Figure 4) is a cyclic polymerization very similar to that calculated in the formic acid case. The system interacts with the surface using two H bonds (1.904 and 2.007 Å), the upper molecule being bonded to the acids only, not directly to ice, the cluster−water

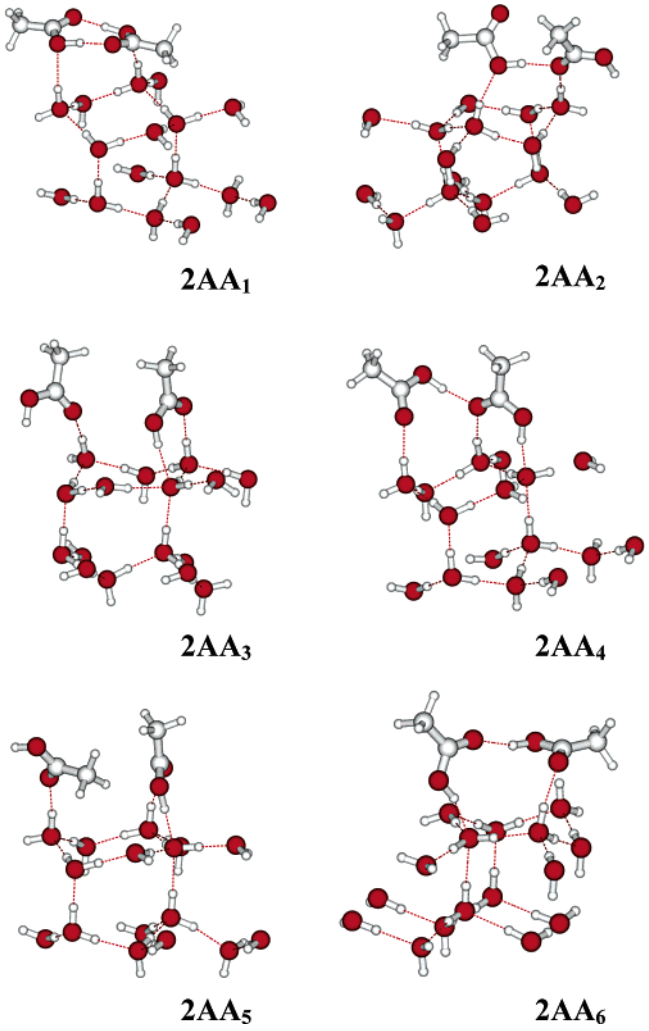

Figure 3. Acetic acid dimers adsorbed on ice.

TABLE 1: Comparison of the Respective Energies of the Systems Described in the Text; the Reference Names in the First Column Are the Same as those In Figures 3−6[a]

system	energy (Hartree)	relative energy (kJ mol^{-1})	cohesive energy (kJ mol^{-1})	adsorption energy ΔE_{BE} (kJ mol^{-1})
H_2O + ice	−291.643280			−64.7
AA + ice	−320.164138		−55.2	−68.8
$2AA_1$	−365.849022	0	−56.1	−38.0
$2AA_2$	−365.846323	7.1	−55.7	−121.6
$2AA_3$	−365.845394	9.5	−55.6	
$2AA_4$	−365.842623	16.8	−55.2	
$2AA_5$	−365.839711	24.4	−54.8	
$2AA_6$	−731.671454	34.9	−54.2	
$3AA_1$	−411.525810	0	−55.8	−95.5
$3AA_2$	−411.523059	7.2	−55.4	
$3AA_3$	−411.519605	15.6	−55.0	
$3AA_4$	−411.517514	21.8	−54.7	
$3AA_5$	−411.516594	24.2	−54.5	
$3AA_6$	−411.513894	31.3	−54.2	
AAH_1	−337.318027	0	−55.0	−45.1
AAH_2	−337.315961	5.4	−54.7	
AAH_3	−337.315696	6.1	−54.7	
AAH_4	−337.308218	25.7	−53.6	
$2AAH_1$	−383.003943	0	−56.0	−91.5
$2AAH_2$	−382.995202	22.9	−54.8	−57.1
$2AAH_3$	−382.994494	24.8	−54.7	

[a] The cohesive energies are calculated using eq 2.

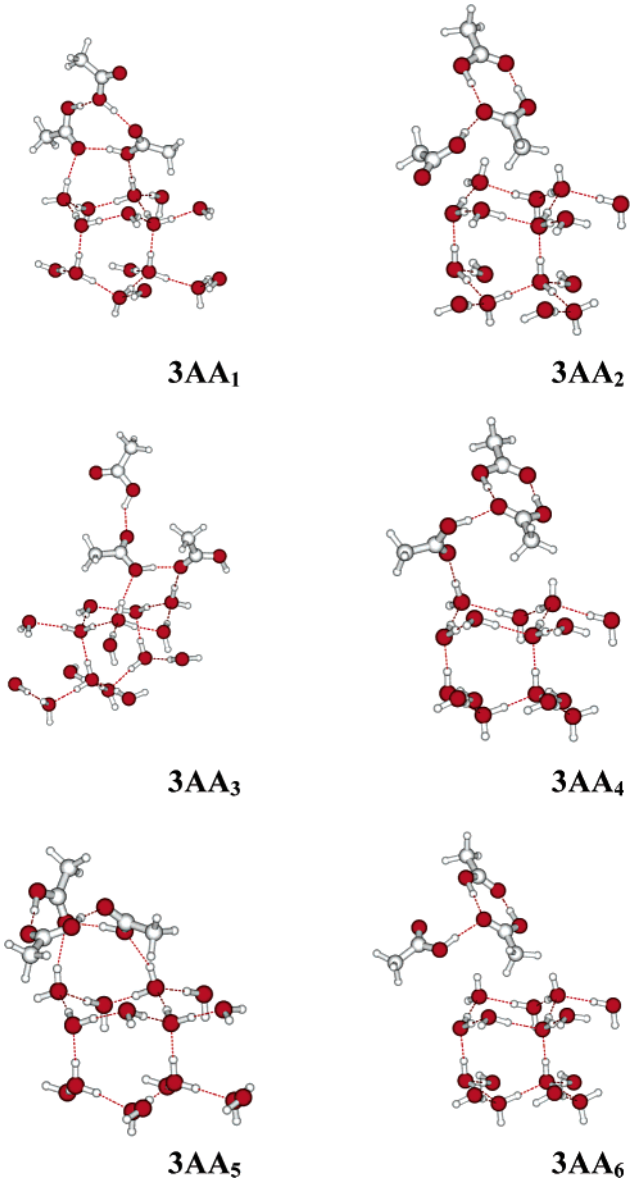

Figure 4. Acetic acid adsorbed on ice as trimers.

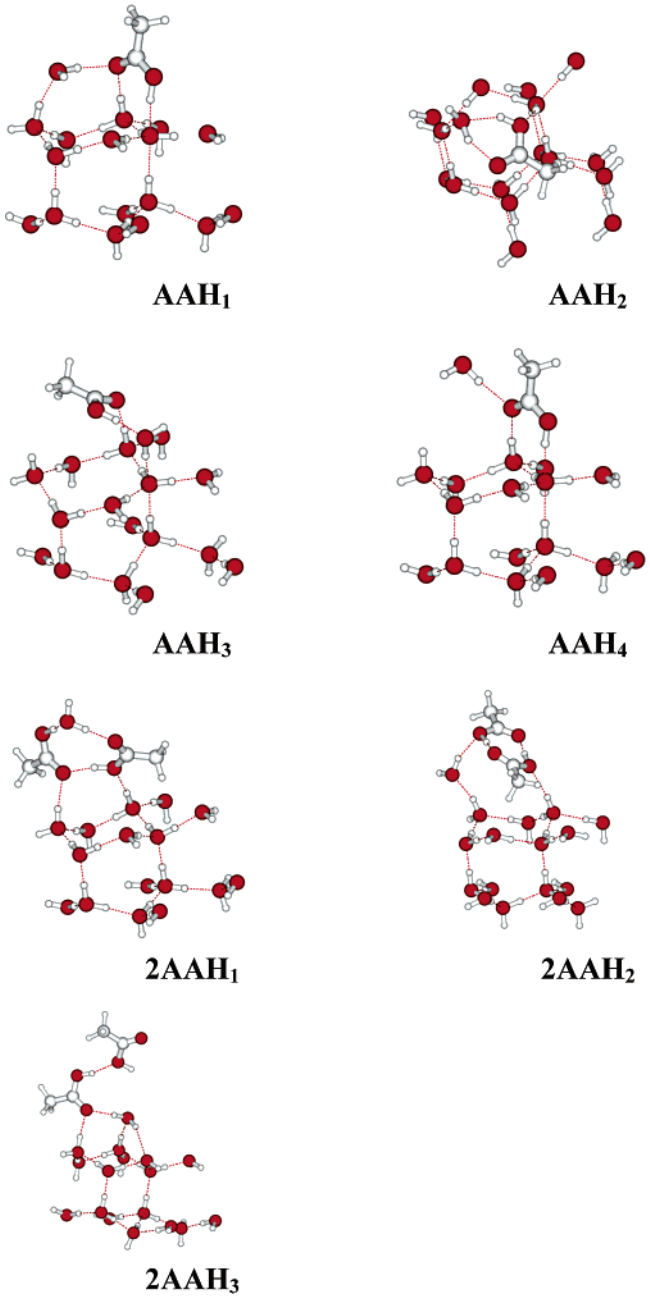

Figure 5. Adsorption on ice of acetic acid associated to one water molecule.

binding energy is −96.5 kJ mol^{-1}. Three AAs is the maximum number of molecules that can be adsorbed on the current ice crystal working cell; within this level approximation it must be considered that monolayer completion is achieved. Therefore, this high adsorption energy must be compared with the previous ones with caution because the adcluster−adcluster interactions could have a lateral contribution.

The other trimer structures are 2 + 1 structures (cyclic C_{2h}-like + 1 AA), they correspond to higher energies, the energy of one of them ($3AA_2$) is only 7.2 kJ mol^{-1} higher.

C. Hydrates. Even at low temperatures, dynamical exchanges occur between the gas phase and the ice surface, some water molecules desorb and some others adsorb. These processes are in competition with acetic acid adsorption and interfere on the AA film formation on ice. The four most stable configurations associating one acid and one water molecules reported in Figure 5 and Table 1, numbered from AAH_1 to AAH_4, are included in an energy range of 25.7 kJ mol^{-1}. The most stable one (AAH_1) corresponds to a complex−ice surface interaction energy of −45.1 kJ mol^{-1} and it involves three H bonds. AAH_2 is a slight distortion of the gas-phase monohydrate, and the adsorbed complex is bonded to the surface by two hydrogen bonds (1.891 and 1.998 Å); the intra-complex H bonds are shorter: 1.770 and 1.786 Å (1.710 and 1.814 Å in the gas phase).

The most stable adsorbed hydrated AA dimer ($2AAH_1$) is cyclic and is associated with an adsorption energy of −91.5 kJ mol^{-1} (same comment on the adsorption energy value as in the previous paragraph); it is the adsorbed form of Chocholousova et al.'s *ac1w* complex.[2] The intermolecular distances are very similar, slightly shorter in the present calculation, 1.508 and 1.650 Å for water−AA, compared with 1.58 and 1.72 Å, and 1.643 Å in lieu of 1.69 Å in isolated Chocholousova's dimer. The other two structures are 22.9 and 24.8 kJ mol^{-1} higher in energy. $2AAH_2$ is a 2 + 1 type complex and $2AAH_3$ is the starting point of an acetic acid syn chain perpendicular to the ice surface.

D. Comparative Stabilities of the Adsorbed Complexes. Comparing the results of the different paragraphs of this section, we can suggest a quantum scenario at temperature of 0 K for

the processes occurring on the ice surface when water and acetic acid are in competition, using the tool of cohesive energy. From the values reported in Table 1, it can be deduced that the preferred adsorbed structure is the C_{2h} dimer in very close competition with the cyclic hydrated dimer $2AAH_1$. Then comes the pure cyclic trimer $3AA_1$ whose energy is very close to $2AA_2$, which is an open dimer.

Nevertheless, the respective cohesive energies are relatively close one to another; therefore, the experimental conditions can impose a configuration not necessarily the most stable from the quantum point of view. Comparison between MIES spectra and quantum DOS calculation provides great help in this problem.

It has been shown[20,21] that the MIES signal is directly proportional to the electronic density of states of the system and it is more precisely sensible only to the first layer of the solid. In the present case the first layer consists of adsorbed acetic acid oligomers or complexes of AAs and water molecules. The experimental conditions are described in Paper II, and the spectra are analyzed therein. In the present contribution, we wish only to compare the quantum DOS associated with the adsorbed systems listed in Table 1 to MIES.

For this purpose, the projected adsorbed system DOS is renormalized, as well as the experimental DOS corresponding to Figures 8 and 9 of Paper II. The origin of energy is taken at the higher experimental peak (peak 3 in Figure 8 of Paper II); the intensity of this peak is also taken as the intensity unit. The result of this transformation is displayed in Figure 6 for the most probable systems.

The projected DOS of AA, $2AA_1$, and $3AA_1$ are characterized by a very weak peak 1 compared to experiment. This indicates that the acetic acid is not adsorbed as a single molecule or a pure AA C_{2h} dimer or a cyclic trimer. The $2AA_2$ DOS is not displayed or discussed because it looks very different form the MIES.

However, the DOS of acetic acid coadsorbed with a water molecule in the AAH_1 configuration is more similar to MIES, whereas AAH_2 is not considered for the same reason as $2AA_2$. A least, it appears from Figure 6 that the simulations closest to experiment are $2AAH_1$, $2AAH_2$, and $3AA_2$. The last two correspond to the cyclic C_{2h} dimer perturbed by a coadsorbed molecule, AA or H_2O.

This qualitative analysis can made more quantitative in calculating the mean distance between the two curves, theoretical and experimental in normalized units. This distances are 0.168 for $2AAH_1$ and $2AAH_2$, 0.169 for $3AA_2$, 0.171 for AAH_1, 0.203 for $2AA_1$ and $3AA_1$, the larger one is 0.232 associated to AA displayed in Figure 2.

Of course this analysis must be seen in the light of the results obtained with the other experimental techniques, UPS, FTIR, and TPD, employed in Paper II, but the combined quantum−MIES analysis leads to the conclusion that formic acid adsorbs on the ice surface in cyclic C_{2h} dimer. This dimer's DOS is perturbed by the coadsorbed species' (H_2O or AA) lateral interaction; it is shown in Paper II that this analysis is consistent with FTIR results.

IV. Water Adsorption on Acetic Acid

A. Solid Acetic Acid. Several authors have suggested an experimental crystal structure of acetic acid; the starting point of the present calculation is the neutron diffraction structure proposed by Jönsson.[22] The system is orthorhombic with unit cell parameters $a = 13.225$ Å, $b = 3.963$ Å, and $c = 5.762$ Å associated to the space group $Pna2_1$. The stability of the crystalline acetic acid is ensured by hydrogen bonds along the

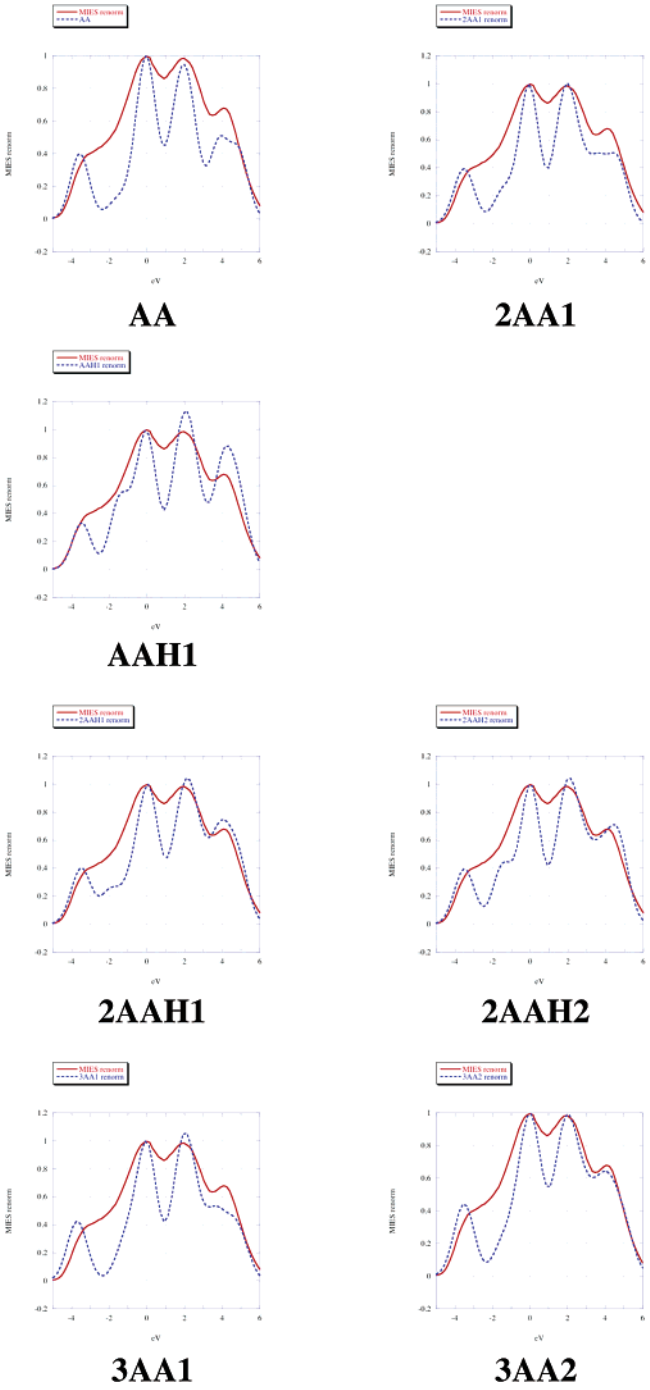

Figure 6. Comparison of the quantum and MIES density of states (DOS) for some of the calculated most stable structures. The spectra have been renormalized taking the highest MIES peak as origin of energy and unit of intensity; the equivalent is done on the DFT one.

catemer patterns and dispersion forces between the chains. The PBE DFT functional provides a fairly good representation of the first contribution. It is very well known that the dispersion contribution cannot be described correctly in this context. Therefore, it would not be reasonable to consider optimization of the crystal parameters here: during the quantum minimization of the unit cell, only the atomic positions were optimized without symmetry constraint, thus keeping the experimental lattice parameters unchanged.

The structure represented in Figure 7 is compared with experiment in Table 2, with the atom numbering taken from Jönsson. It can be seen that despite the lack of optimization of the lattice constants, the agreement is globally good except for

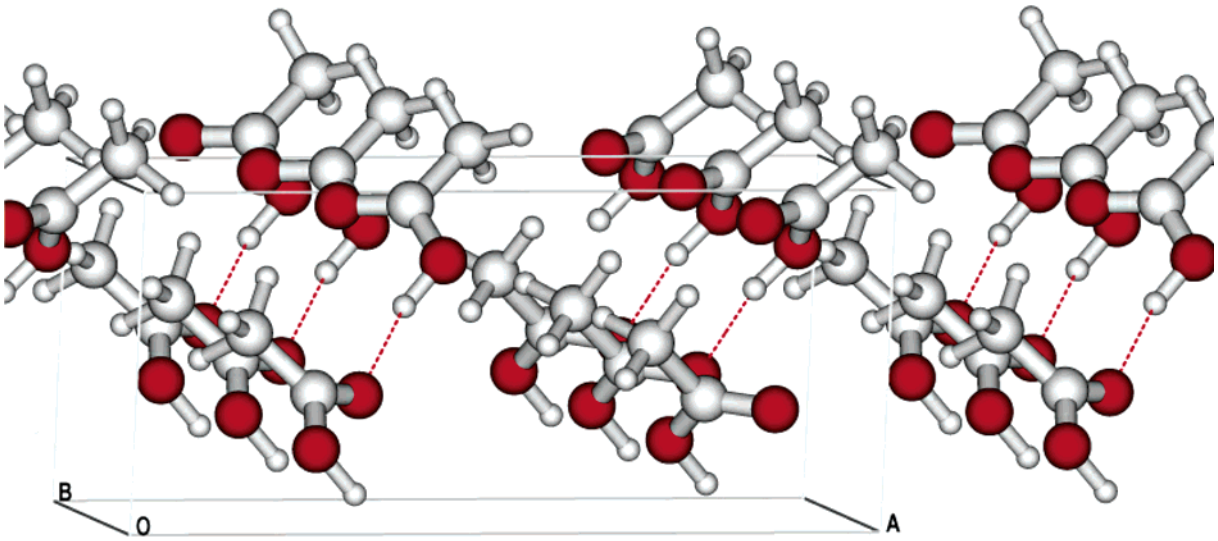

Figure 7. Structure of the crystalline syn form of acetic acid.

TABLE 2: Structural Parameters of Crystalline Syn Acetic Acid from Neutron Diffraction,[22] PBE/PW Calculation for the Crystal and the Isolated Molecule[a]

	Jönsson[22]	PBE/PW crystal	PBE/PW gas	Rovira et al.[23] crystal
C(1)−O(1)	1.321 [1.330]	1.319	1.367	1.325
C(1)═O(2)	1.206 [1.215]	1.238	1.217	1.249
C(1)−C(2)	1.501	1.484	1.500	1.487
C(2)−H(2)	1.078 [1.139]	1.095	1.098	1.095
C(2)−H(3)	1.050 [1.119]	1.083	1.092	
C(2)−H(4)	1.052 [1.140]	1.097	1.098	
O(1)−H(1)	1.011 [1.014]	1.017	0.982	1.046
O(2)···H(1)	1.642	1.679		1.548
O(1)···O(2)	2.631	2.681		
O(2)···H(2)	2.409	2.702		2.271
C(2)···O(2)	3.429	3.685		
O(1)−C(1)═O(2)	121.9	122.2	122.1	121.7
C(2)−C(1)−O(1)	113.2	115.4	111.4	112.0
C(2)−C(1)═O(2)	124.9	122.1	126.5	124.1
C(1)−C(2)−H(2)	107.7	109.9	109.9	
C(1)−C(2)−H(3)	108.9	114.5	109.9	
C(1)−C(2)−H(4)	112.3	103.5	109.9	
H(2)−C(2)−H(3)	113.3	112.3	106.7	
H(2)−C(2)−H(4)	108.1	106.1	110.2	
H(3)−C(2)−H(4)	108.6	109.7	110.2	
C(1)−O(1)−H(1)	110.5	111.5	106.0	
O(1)−H(1)···O(2)	164.8	166.9		
C(1)═O(2)···H(1)	129.1	112.1		
C(2)−H(2)···O(2)	157.4	149.1		
C(1)═O(2)···H(2)	116.8	103.9		

[a] Rovira et al.'s[23] results are given in the last column.

the two hydrogen-bond angles C (1)−O (2)H···(1) and C (1)−O (2)···H (2), which are about 10° underevaluated. Compared with the isolated molecule structure obtained using the same quantum method, the only noticeable change concerns the two CO bonds lengths: C═O is shorter and C−O is longer, underlining that PBE/PW tends to overestimate the hydrogen-bond interaction.

Rovira et al.[23] recently published a Car−Parrinello comparative study of the syn and anti forms of crystalline AA. They chose the BP DFT functional, empirically supplemented by fitted dispersion terms. Their results are not significantly different from ours. The difference between C−O and C═O bonds is similar (0.076 Å to 0.081 Å) but the latter is more overestimated than ours and their carboxyl group angles are slightly closer to experimental values.

Nonetheless, our purpose is not to propose a new AA crystal structure derived from quantum calculation but to identify the most characteristic reactive sites concerning water molecule adsorption. Hence, four two-layer slabs were extracted and optimized from thus bulk solid by simply cutting along characteristic crystal directions and including a vacuum above the surface large enough to avoid slab−slab interactions (c = slab + vacuum thickness = 20 Å).

(i) The [110] working cell parameters are 5.762 and 13.806 Å and 48 atoms. The syn catemer chains are perpendicular to the surface plane, which consists of series of C═O···CH_3···−OH··· valley patterns. Optimization has little effect on this surface, the O···HO bonds evolves from 1.635 to 1.685 Å to 1.697−1.610 Å.

(ii) The [011] slab features mainly methyl groups and also includes 48 atoms with parameters 13.225 and 6.993 Å. The catemer chains are parallel to the surface plane. In respect to the bulk structure, the H bonds are noticeably shorter: 1.514 and 1.470 in place of 1.600 Å.

(iii) The 48 atom [101] slab has parameters of 14.426 and 3.963 Å. The catemer chains end below the surface plane at an angle of about 45°; therefore, even if the surface is also hydrophobic, large valleys between the methyl group alignments leave an easy access to the free AA carboxyls. The slab relaxation implicates a slight increase of the H bond (1.698−1.720Å). This long bond length enables rotation of some monomers and then the exchange of proton between two neighbors; as a consequence, one AA of two is now in a gauche form and the other one remains in the syn configuration.

(iv) The parameters of the [111] unit cell are 13.806 and 6.993 Å including a larger number of atoms than before, that is, 56. From an electrostatic standpoint, the surface structure is composed of hydrophobic methyls and hydrophilic hydroxyls. The hydrogen hydroxyls are directed toward the inside of the solid, then the oxygen dangling electron doublets point toward the vacuum and are easily accessible to a reactive adsorbent. The optimization effect is to significantly shorten the three H bonds from (1.606, 1.612, and 1.693) to 1.492 Å and 1.457 Å, the third one being on the contrary slightly longer: 1.763Å.

From this short discussion, it can be concluded that even if the surface sampling is restricted for obvious technical reasons, it is large enough to ensure that the most important reactive sites are represented in this panel.

B. Water Molecule Adsorption. The adsorption of water on the surface planes described in the previous section was calculated by complete minimization of the entire system. The results summarized in Table 3 and Figure 8 show that four

TABLE 3: Adsorption Energy of One Water Molecule on Different Acetic Acid Surfaces

structure	ΔE_{BE} (kJ mol^{-1})
110_A	−37.3
011_A	−12.5
011_B	−13.4
101_A	−46.1
101_B	−41.0
111_A	−41.3
111_B	−19.2
111_C	−12.1

systems are associated with significant adsorption energies ranging from −37.3 to −46.1 kJ mol^{-1}. The first point is that the water molecule is adsorbed more strongly on water ice than on AA surfaces; this competition plays in favor of the formation of water clusters on the AA solid.

(i) In the 110_A structure, the H_2O molecule is singly H bonded to one AA (1.811 Å) through the carbonyl group.

(ii) Because the [011] surface is largely hydrophobic, it produces zero or very small interaction energies with water.

(iii) The [101] surface is significantly more reactive, and two table structures were found. In 101_A, the water molecules are bonded to their two neighboring acid carbonyl groups (bond lengths 1.724 and 2.022 Å), whereas in the 101_B structure they are adsorbed on the other side of the valley lying between the acid chains. The longer H_2O−AA bonds (1.775 and 2.118 Å) reflect a weaker interaction, which is compensated by better water−water stabilization, and the adsorption energy is not significantly different from 101_A.

(iv) On the [111] surface, the only stable structure is finally the first one, where the H_2O−AA interaction is ensured by a single hydrogen bond (1.826 Å), the methyl group's repulsion at last makes the other potential sites unreachable.

V. Discussion and Conclusions

The main motivation of this paper was to model the water−acetic acid interface in solid state through the acid adsorption on water ice and water adsorption on solid acid. These results are compared with infrared and electronic spectroscopy studies in the appended theory−experiment paper.[13]

However, the present results can be criticized on several points. The most important is that the PBE/PW method tends to shorten the H-bond lengths and could then be suspected of overestimating them. Moreover, PBE, like most of the other first-principles DFT, poorly represents the dispersive contributions. Also, the objection can be raised that the zero-point energy correction cannot be done.

These disadvantages are largely balanced by representing the substrate as an infinite pseudo 2D medium, that is, the surface of a solid. Because, besides the differences between the competing systems, energies are often not very high, the discussion must include these considerations and develop at a semiquantitative level rather than comparing the last digit of their values.

The first steps in the formation of an AA film on the ice surface are controlled by the competition between AA−H_2O, AA−AA, and H_2O−H_2O relative interactions, according to temperature and concentration in the acetic acid on the surface.

Within the limits of our method, Table 1 summarizes the most probable processes. The dispersion of the cohesive energies does not look very significant but it must be kept in mind that these values must be multiplied by the number of molecules in the crystal unit cell. In this context, and at 0 K temperature, the table clearly shows that the preferential mode of adsorption is AA as a cyclic dimer (C_{2h}-like). However, if some water molecules are present (as a result of the surface dynamics for instance) then this model is in close competition with the coadsorption model referred to as $2AAH_1$, that is, a three-items cyclic structure associating two AAs and one water. In addition, the $2AA_2$ structure (which does not involve a cyclic dimer) is only 7.1 kJ mol^{-1} less stable, and at this level of approximation it cannot be excluded completely although its DOS looks very different from the MIES signal.

When the adsorbed cluster grows, the water molecule's inclusion tends to be eliminated and the most stable structure could be the cyclic $3AA_1$ trimer or according to comparison with MIES the 2 + 1 trimer $3AA_2$. Given the size our crystal cell, three is the largest number of acetic acid molecules that can be adsorbed; beyond this, the AA film grows as an amorphous multilayer film composed of dimers, trimers, and maybe more complex. This analysis is supported by comparison of the quantum DOSs with MIES; interpretations of other experimental results are discussed in Paper II.

The way the amorphous acid film can evolve into a crystalline structure remains beyond the realm of our method. At this point of the discussion and taking into consideration other spectroscopic results analyzed in Paper II, the hypothesis of an amorphous film composed mainly of dimers is the most realistic.

Without performing heavy calculations, this film cohesion must be due to van der Waals-type interactions because all of the possible sites of hydrogen bonds are normally saturated. Therefore, to minimize the steric repulsions generated by the methyl groups, two dimers must be stacked one above the other in a position similar to that shown in the "*artistic*" view of Figure 9. In such a situation, if the two subsystems are close enough, a proton can be transferred from the lower-part system to the higher-part one. This could induce a joint process inducing the transfer of another proton in the two subsystems in parallel with the construction of a new network of hydrogen bonds and reorganization of the layer. We have shown in previous papers[24,25] that such proton transfers could be done at a very low cost in energy.

In any event, we have demonstrated that the water molecules can be incorporated into the crystalline acid film along the catemer chains through one or two hydrogen bonds. This could form the first step of a water film growing on solid AA. On the [101] surface, the large valley between the catemer chains is bordered by C═O groups and the 101_A and 101_B structures represent the adsorption mode of water on each side of the valley. Once these sites are saturated, the AA surface is passivated by the hydrophobic methyl groups and the water film could grow only through water−water interaction. In the 111_A case, the situation is even worse from this point of view because only one site is available and it is embedded between rows of dangling methyls.

From these considerations on the water−acetic acid interface, we can conclude that acid on water and water on acid each tend to organize themselves as homogeneous phases excluding the other partner.

A recent combined experiment−molecular dynamics study was devoted to AA adsorption on water ice by Picaud et al.[6] We have already pointed out our diverging views with Compoint et al.[10] also published by the same group. From our calculations, it appears that the AA−AA interaction is noticeably stronger than the AA−H_2O one. Therefore, the cyclic dimer is less bonded to the ice surface than the open dimer because the global system stability is covered in the first case by a larger acid−

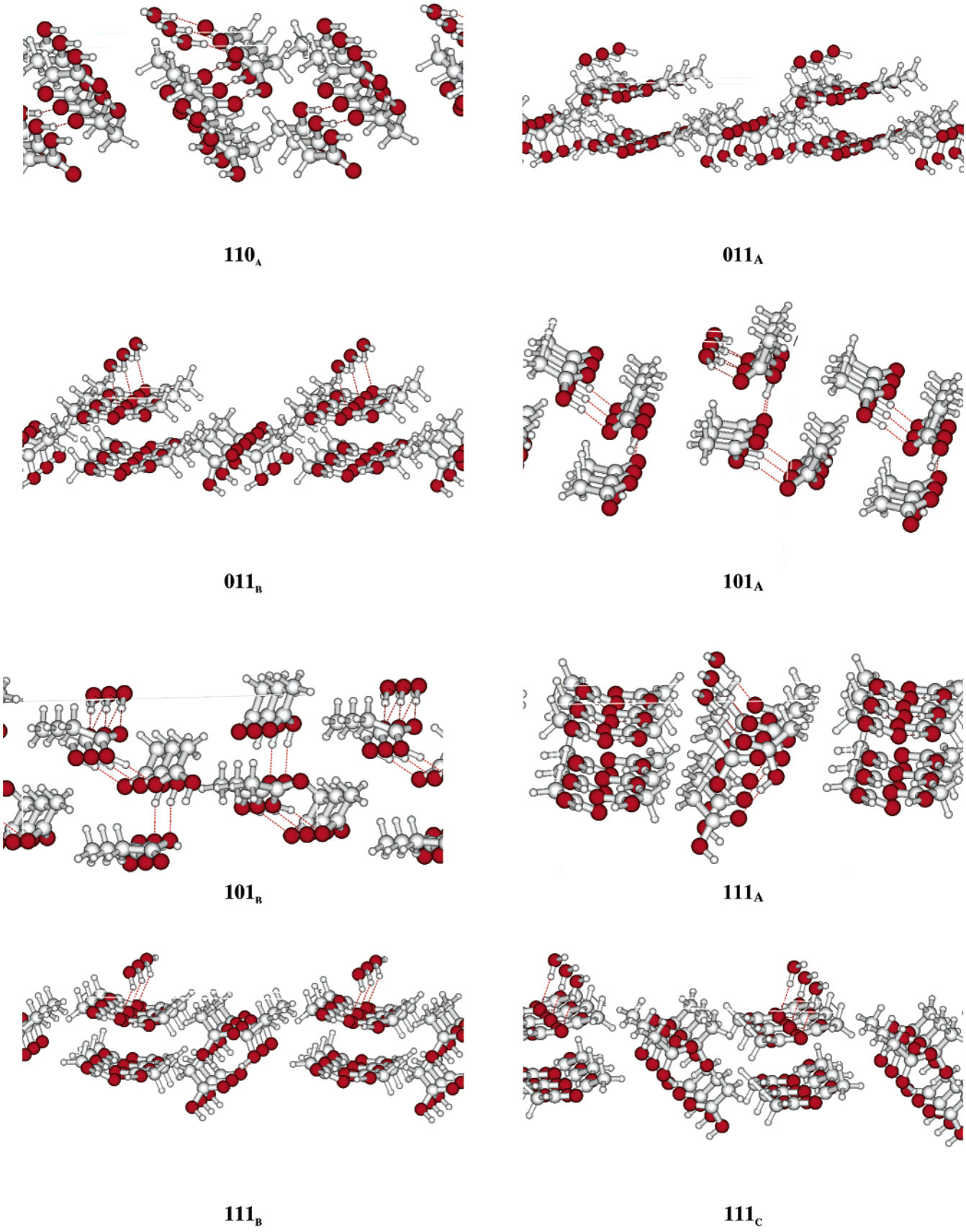

Figure 8. Water molecule adsorption on acetic acid surfaces cut out of the bulk represented in Figure 7.

acid contribution. Therefore, the cyclic dimer adsorption energy (−38.0 kJ mol^{-1}) is smaller than the open dimer adsorption as a whole (−121.6 kJ mol^{-1}, −115.7 kJ mol^{-1} for Compoint et al.) and besides, the adsorption energy of one AA from the adsorbed complex is even larger (−151.6 kJ mol^{-1}). The experimental adsorption enthalpy (−33.5 kJ mol^{-1}) reported in Picaud et al.'s paper is completely consistent with this analysis and is remarkably close to our adsorption energy of the cyclic dimer (−38.0 kJ mol^{-1}). This analysis is compared to the TPD results in Paper II.

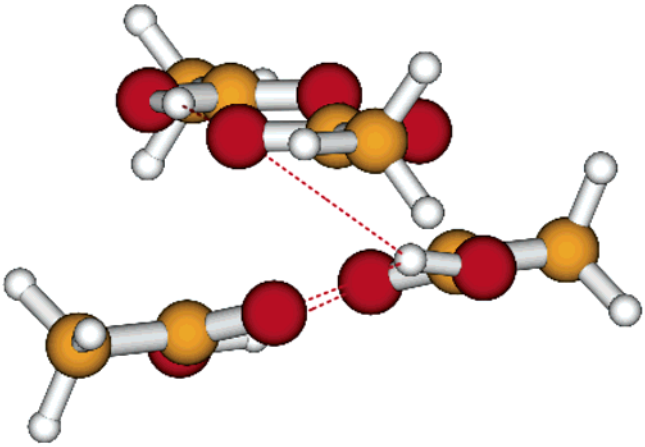

Figure 9. Artistic view showing how two cyclic acetic acid dimers could be transformed into an open chain structure by proton transfer.

Acknowledgment. The Marseille (PIIM Laboratory) − Clausthal (Prof. V. Kempter group) cooperation was supported by the COST (European CO-operation in the field of Scientific and Technical Research) D19 action. All of the calculations were performed at IDRIS, the CNRS computing Center.

References and Notes

(1) Nakabayashi, T.; Kosugi, K.; Nishi, N. *J. Phys. Chem. A* **1999**, *103*, 8595.
(2) Chocholousova, J.; Vacek, J.; Hobza, P. *J. Phys. Chem. A* **2003**, *107*, 3086.
(3) Génin, F.; Quilés, F.; Burneau, A. *Phys. Chem. Chem. Phys.* **2001**, *3*, 932.
(4) Colominas, C.; Luque, F. J.; Orozco, M. *J. Comput. Chem.* **1999**, *20*, 665.
(5) Sokolov, S.; Abbatt, J. P. D. *J. Phys. Chem. A* **2002**, *106*, 775.
(6) Picaud, S.; Hoang, P. N. M.; Peybernes, N.; Le Calve, S.; Mirabel, Ph. *J. Chem. Phys.* **2005**, *122*, 194707.
(7) Kondo, M.; Shibata, T.; Kawanowa, H.; Gotoh, Y.; Souda, R. *Nucl. Instrum. Methods Phys. Res., Sect. B* **2005**, *232*, 134.
(8) Gao, Q.; Leung, K. T. *J. Phys. Chem. B* **2005**, *109*, 13263.
(9) Gao, Q.; Leung, K. T. *J. Chem. Phys.* **2005**, *123*, 074325.
(10) Compoint, M.; Toubin, C.; Picaud, S.; Hoang, P. N. M.; Girardet, C. *Chem. Phys. Lett.* **2002**, *365*, 1.
(11) Allouche, A. *J. Chem. Phys.* **2005**, *122*, 234703.
(12) Bahr, S.; Borodin, A.; Höfft, O.; Kempter, V.; Allouche, A. *J. Chem. Phys.* **2005**, *122*, 234704.
(13) Bahr, S.; Borodin, A.; Höfft, O.; Kempter, V.; Allouche, A.; Borget, F.; Chiavassa, Th. *J. Phys. Chem. B* **2006** *110*, 8649.
(14) Baroni, S.; Dal Corso, A.; de Gironcoli, S.; Giannozzi, P.; Cavazzoni, C.; Ballabio, G.; Scandolo, S.; Chiarotti, G.; Focher, P.; Pasquarello, A.; Laasonen, K.; Trave, A.; Car, R.; Marzari, N.; Kokalj, A. http://www.pwscf.org/
(15) Laasonen, K.; Pasquarello, A.; Lee, C.; Car R.; Vanderbilt, D. *Phys. Rev. B* **1993**, *47*, 10142.
(16) Manca, C.; Martin, C.; Allouche, A.; Roubin, P. *J. Phys. Chem. B* **2001**, *105*, 12861.
(17) (a) Pisani, C.; Casassa, S.; Ugliengo, P. *Chem. Phys. Lett.* **1996**, *253*, 201. (b) Casassa, S.; Ugliengo, P.; Pisani, C. *J. Chem. Phys.* **1997**, *106*, 8030.
(18) Johnson, C. M.; Tyrode, E.; Baldelli, S.; Rutland, M. W.; Leygraf, C. *J. Phys. Chem. B* **2005**, *109*, 321.
(19) Adélia, J. A.; Aquino, D. T.; Haberhauer, G.; Gerzabek, M. H.; Lischka, H. *J. Phys. Chem. A* **2002**, *106*, 1862.
(20) Ochs, D.; Maus-Friedrichs, W.; Brause, M.; Günster, J.; Kempter, V.; Puchin, V.; Shluger, A.; Kantorovich, L. *Surf. Sci.* **1996**, *365*, 557.
(21) Kantorovich, L. N.; Shluger, A. L.; Sushko, P. V.; Günster, J.; Stracke, P.; Goodman, D. W.; Kempter, V. *Faraday Discuss.* **1999**, *114*, 173.
(22) Jönsson, P.-G. *Acta Crystallogr., Sect. B* **1971**, *27*, 893.
(23) Rovira, C.; Novoa, J. J. *J. Chem. Phys* **2000**, *113*, 9208.
(24) Ferro, Y.; Allouche, A.; Kempter, V. *J. Chem. Phys.* **2004**, *120*, 8683.
(25) Allouche, A.; Couturier-Tamburelli, I.; Chiavassa, T. *J. Phys. Chem. B* **2000**, *104*, 1497.